Observed Accuracy of Point-Tested and Galerkin Implementations of the Volume EFIE for Dielectric Targets

Andrew F. Peterson

School of Electrical and Computer Engineering
Georgia Institute of Technology, Atlanta, GA. 30332-0250, USA
peterson@ece.gatech.edu

Abstract **─** Galerkin testing in method-of-moments procedures is defined as the use of the same set of functions as both basis functions and testing functions to construct a linear system from a continuous equation. There is a widespread belief that Galerkin testing enhances the accuracy of numerical results, and this has been shown to be true under certain conditions for surface integral equation formulations. This property is investigated for the volume electric field integral equation (EFIE) applied to dielectric bodies. The relative accuracy obtained in internal fields and scattering cross section for Galerkin and for point testing schemes is compared for a variety of target sizes and materials. In many cases, the point-tested results converge at the same rate as the Galerkin results and are more accurate.

Index Terms **─** Dielectric targets, method of moments, numerical techniques, radar cross section.

I. INTRODUCTION

There are numerous applications requiring accurate numerical solutions for electromagnetic fields in the presence of heterogeneous dielectric bodies. Volume integral equation formulations offer one avenue to approach these problems, and are of interest in conjunction with fast iterative solvers due to their relatively low matrix condition numbers. Formulations based on both the electric field integral equation (EFIE) and the magnetic field integral equation (MFIE) using tetrahedral cells in 3D have been proposed [1-7]. The EFIE approaches impose the integral equation using "Galerkin" testing, where testing functions that are identical to the basis functions are used to enforce the equations and create a linear system. This type of testing scheme imposes a cost in the form of additional integrations that must be carried out to produce the system of equations. Galerkin testing offers the advantage that it produces a symmetric matrix for EFIE formulations, and may make it easier to compute the entries of the system matrix by distributing derivatives and thereby limiting the order of the Green's function singularity. However, there is also a widespread belief that Galerkin testing is associated with a variational principle that enhances the accuracy of the numerical results, specifically the far fields and scattering cross section (SCS) [8-9].

For surface EFIE formulations involving scattering from conducting targets, the SCS accuracy converges at a faster rate than the surface current density when Galerkin testing is used with mixed-order divergence-conforming basis functions [10]. Galerkin-tested results with these basis functions also show faster convergence rates and improved accuracy for SCS compared to point-tested results [10]. However, this "super-convergence" does not happen for all equations and all basis function types [11]. Furthermore, to the author's knowledge, this phenomenon has not been investigated for volume integral equations.

The following considers the widely-used EFIE-D formulation proposed in [1], where the electric flux is represented by mixed-order divergence-conforming Schaubert-Wilton-Glisson (SWG) basis functions. Results obtained using a Galerkin testing scheme to enforce the EFIE are compared with results obtained using point testing in the center of the cell faces. The theory of variational techniques [9] suggests that the accuracy of internal fields obtained by the two approaches should be

Submitted On: October 15, 2014
Accepted On: December 11, 2014

similar, but that the accuracy of the SCS will be improved by Galerkin testing. However, results suggest that this is not the case for most of the examples considered. Often, point testing produces more accurate SCS results than Galerkin testing. Preliminary results of this study were reported in [12-13].

II. THE POINT TESTED EFIE-D FORMULATION

Details of the point-tested EFIE-D formulation are not reported in the literature, so the expressions arising from that scheme that are summarized in this section. The EFIE can be expressed:

$$\bar{E}^{inc} = \bar{E}^{tot} + j\omega\mu_0\left(\bar{J} * \frac{e^{-jkr}}{4\pi r}\right) + \frac{1}{\varepsilon_0}\nabla\left(\rho_e * \frac{e^{-jkr}}{4\pi r}\right), \quad (1)$$

where the asterisk denotes spatial convolution, ω is the radian frequency, μ_0 and ε_0 are the permeability and permittivity of the background medium, and $k = \omega\sqrt{\mu_0\varepsilon_0}$ is the wavenumber of the background medium. The electric flux, polarization current, and polarization charge densities are represented by:

$$\bar{D}^{tot}(\bar{r}) \cong \sum_{n=1}^{N_f} D_n \bar{f}_n(\bar{r}), \quad (2)$$

$$\bar{J} \cong j\omega\sum_{n=1}^{N_f} D_n \kappa(\bar{r}) \bar{f}_n(\bar{r}), \quad (3)$$

and

$$\rho_e \cong -\sum_{n=1}^{N_f} D_n \kappa(\bar{r}) \nabla \bullet \left\{\bar{f}_n(\bar{r})\right\} - \sum_{n=1}^{N_f} D_n \left\{\kappa_n^- - \kappa_n^+\right\}\delta(\bar{r} - \bar{r}_n), \quad (4)$$

where $\bar{f}$ denotes an SWG basis function straddling two tetrahedral cells T_n^+ and T_n^- adjacent to face n [1], and $\kappa = (\varepsilon_r - 1)/\varepsilon_r$ denotes the contrast ratio of the appropriate cell, where ε_r is the relative permittivity of that cell. The point-matched approach employs a Dirac delta test function:

$$\bar{T}_m(\bar{r}) = \hat{u}_m \delta(x - x_m)\delta(y - y_m)\delta(z - z_m), \quad (5)$$

where (x_m, y_m, z_m) denotes the center of face m and $\hat{u}_m$ is a normal vector to that face pointing from cell T_m^+ to cell T_m^-. However, since the total electric field exhibits a jump discontinuity at a dielectric boundary, the EFIE must be tested slightly to one side of such an interface, at a point where the total, scattered, and incident fields are all well-defined. For uniqueness, we will test slightly to the T_m^+ side of face m.

Point testing produces the system of equations **ZD** = **E**, where the entries of the system are:

$$\begin{aligned} Z_{mn} &= \frac{1}{\varepsilon_0 \varepsilon_{rm}^+} \hat{u}_m \bullet \bar{f}_n(\bar{r}_m) \\ &- \hat{u}_m \bullet \frac{k^2}{\varepsilon_0}\left\{\kappa_n^+ \iiint_{T_n^+} \bar{f}_n(\bar{r}')\frac{e^{-jkR}}{4\pi R}dv' + \kappa_n^- \iiint_{T_n^-} \bar{f}_n(\bar{r}')\frac{e^{-jkR}}{4\pi R}dv'\right\}_{\bar{r}_m} \\ &- \hat{u}_m \bullet \frac{1}{\varepsilon_0}\nabla\left\{\frac{a_n\kappa_n^+}{V_n^+}\iiint_{T_n^+}\frac{e^{-jkR}}{4\pi R}dv' - \frac{a_n\kappa_n^-}{V_n^-}\iiint_{T_n^-}\frac{e^{-jkR}}{4\pi R}dv'\right\}_{\bar{r}_m} \\ &- \frac{1}{\varepsilon_0}\left\{\kappa_n^- - \kappa_n^+\right\}\hat{u}_m \bullet \nabla\left\{\iint_n \frac{e^{-jkR}}{4\pi R}dS'\right\}_{\bar{r}_m \text{ in } T_m^+}, \end{aligned} \quad (6)$$

and the excitation vector is:

$$E_m = \hat{u}_m \bullet \bar{E}^{inc}(\bar{r}_m). \quad (7)$$

The evaluation of the first and second expressions in (6) is straightforward; in the latter case there is a $1/R$ singularity at the observer that can be handled by the usual singularity cancellation procedures. The third term in (6) may be expressed as:

$$\begin{aligned} Z_{mn}^Q &= \frac{1}{\varepsilon_0}\frac{a_n\kappa_n^+}{V_n^+}\iiint_{T_n^+}\hat{u}_m \bullet \hat{R}\left\{(1 + jkR)\frac{e^{-jkR}}{4\pi R^2}\right\}dv'\Bigg|_{\bar{r}_m} \\ &- \frac{1}{\varepsilon_0}\frac{a_n\kappa_n^-}{V_n^-}\iiint_{T_n^-}\hat{u}_m \bullet \hat{R}\left\{(1 + jkR)\frac{e^{-jkR}}{4\pi R^2}\right\}dv'\Bigg|_{\bar{r}_m}. \end{aligned} \quad (8)$$

These integrals contain $1/R^2$ singularities at the observer, but since they are volume integrals they are integrable and can also be handled by singularity cancellation transformations.

Finally, when the observation point is located on the source face, the final expression in (6) may be evaluated analytically to produce:

$$\begin{aligned} Z_{mn}^S &= -\frac{1}{\varepsilon_0}\left\{\kappa_n^- - \kappa_n^+\right\}\iint_n \hat{u}_m \bullet \hat{R}\left\{(1 + jkR)\frac{e^{-jkR}}{4\pi R^2}\right\}dS'\Bigg|_{\bar{r}_m \text{ in } T_m^+} \\ &= -\frac{1}{2\varepsilon_0}\left\{\kappa_n^- - \kappa_n^+\right\}. \end{aligned} \quad (9)$$

In summary, for a point-tested EFIE, the matrix entries are well defined and bounded and may be computed without difficulty. Integrals are performed using adaptive quadrature to an accuracy of at least 3 decimal places.

III. NUMERICAL RESULTS

A variety of results were computed for homogeneous spherical targets of different size and permittivity, using a series of tetrahedral-cell meshes ranging from 32 cells (80 faces) to 3383 cells (7067 faces). The error in each result was determined using exact solutions obtained from the eigenfunction series. The 2-norm error in the scattering cross section is defined:

$$E = \frac{\sqrt{\frac{1}{N_{angles}} \sum_{n=1}^{N_\theta} \sum_{m=1}^{N_\phi} \sin\theta_m \left| \sigma_{exact}(\theta_m, \phi_n) - \sigma_{numerical}(\theta_m, \phi_n) \right|^2}}{\sigma_{exact, forward}}, \quad (10)$$

while the 2-norm error in the internal electric field is:

$$E = \frac{1}{\varepsilon_r \eta_0} \sqrt{\frac{1}{N_{faces}} \sum_{n=1}^{N_{faces}} \left| \varepsilon_r E_n^{nor} \Big|_{exact} - \varepsilon_r E_n^{nor} \Big|_{numerical} \right|^2}. \quad (11)$$

The SCS error was averaged on a 30 degree grid in spherical angles (θ,ϕ); the error in internal fields was compared at the center of each face in the mesh.

In addition to results obtained from the point-tested EFIE-D and the Galerkin-tested EFIE-D, we also computed results for each target using the Galerkin-tested EFIE-H formulation, which employs solenoidal basis functions for the electric flux [3,7].

As an illustration of typical results, Fig. 1 shows the error in the bistatic SCS versus number of unknowns for a homogeneous dielectric sphere with $ka = 0.6$ and $\varepsilon_r = 10$, averaged over samples taken every 30 degrees in θ and ϕ. For this target, the Galerkin-tested EFIE-D SCS is slightly more accurate than the point-tested EFIE-D SCS, but both are converging at an approximate rate of $O(h^2)$, where h is the average cell dimension. SCS results were observed to converge at an $O(h^2)$ rate for every target considered in this study, for both point-tested and Galerkin results. The SCS produced by the EFIE-H formulation is somewhat more accurate than either EFIE-D result for a given mesh and for a similar number of unknowns. Figure 2 shows the error in the internal electric fields versus the number of unknowns, for $ka = 0.6$ and $\varepsilon_r = 10$, obtained from (11) by averaging over every cell face in the mesh. The point-tested EFIE-D results are slightly more accurate than the Galerkin-tested EFIE-D results, and are similar in accuracy to the EFIE-H results. In this case, the rate of convergence of the internal electric field appears to be somewhere between $O(h)$ and $O(h^2)$.

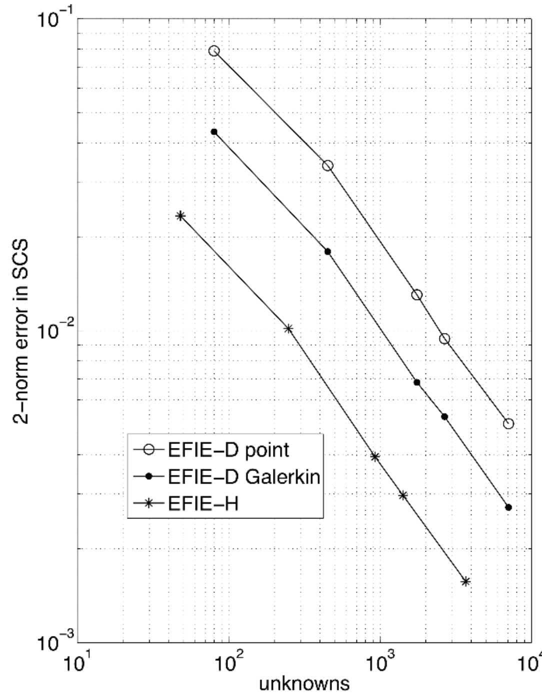

Fig. 1. Error in the SCS for a dielectric sphere with $ka = 0.6$ and $\varepsilon_r = 10.0$.

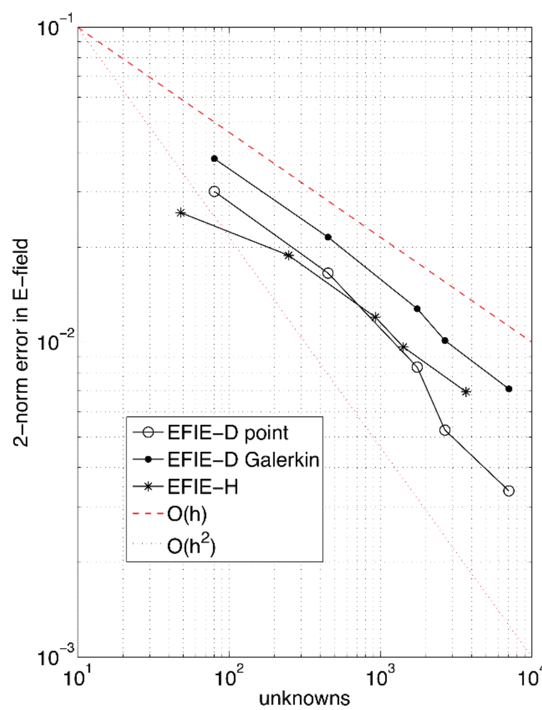

Fig. 2. Error in the internal electric field for a sphere with $ka = 0.6$ and $\varepsilon_r = 10.0$.

Figure 3 shows the error in the SCS versus number of unknowns for a larger sphere with ka = 1.5 and ε_r = 10. For this target, the point-tested EFIE-D SCS is almost an order of magnitude more accurate than the Galerkin-tested EFIE-D SCS, with both converging at an O(h^2) rate. Figure 4 shows the error in the internal electric fields for this target. The point-tested EFIE-D internal field results are more accurate than the Galerkin-tested EFIE-D results. The EFIE-H results exhibit an accuracy between those of the point-tested and Galerkin tested EFIE-D results. In this case, the rate of convergence of the internal electric field appears to be O(h^2) for both point and Galerkin tested approaches.

Table 1 shows the approximate error in the SCS and internal fields for a range of targets, at a common cell density where the average edge length is approximately 0.1 λ_d within the target. For the specific set of models in use, the number of faces (and therefore, the number of unknowns) that corresponds to an average cell edge length of 0.1 dielectric wavelengths is approximately given by:

$$N_{faces} \cong 400(k_0 a)^3 (\varepsilon_r)^{1.5}. \quad (12)$$

We will use unknown level in (12) to standardize accuracy comparisons. These results are extrapolated from error plots similar to those in Figs. 1-4 using (12) to identify the appropriate number of unknowns. Table 2 shows the observed rate of convergence for the electric field in each set of results. The SCS always appears to converge at an O(h^2) rate.

From Table 1 we observe that, at an average edge length of 0.1 λ_d, the point-tested EFIE-D results for internal fields exhibit an error level of approximately 0.007 across a wide range of target parameters. The error level for the Galerkin-tested EFIE-D internal fields for this average edge length is much more variable, and usually at least twice as high as the point-tested errors. For SCS errors, the point-tested results show a trend of lower error as the effective target size grows, while Galerkin-tested SCS results seem to show the opposite. In other words, from these data, it appears that the Galerkin SCS error grows as either k_0a or ε_r increases, despite the cell dimensions being reduced to compensate for the smaller dielectric wavelength.

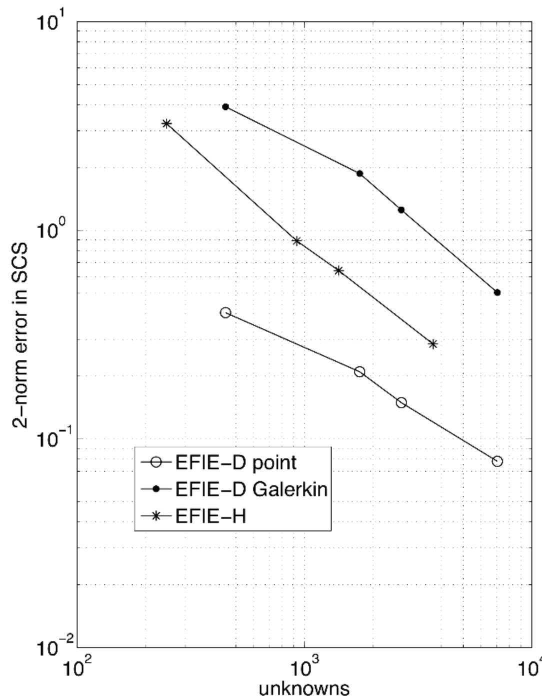

Fig. 3. Error in the SCS for a dielectric sphere with ka = 1.5 and ε_r = 10.0.

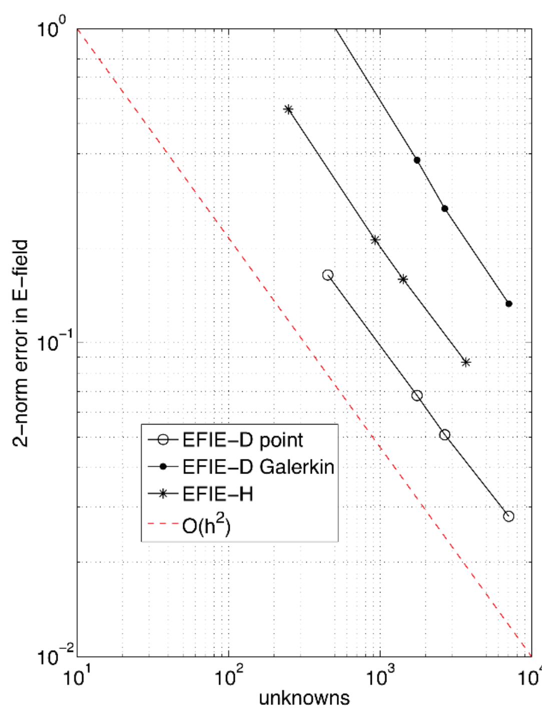

Fig. 4. Error in the internal electric field for a sphere with ka = 1.5 and ε_r = 10.0.

IV. DISCUSSION

For SWG bases, which are fundamentally piecewise-constant functions, the error in the internal fields is expected to converge at an O(h) rate. However, it appears that the field error at the center of the faces of the mesh converges at a superconvergent rate of O(h^2). (A similar effect occurs in numerical solutions of the surface EFIE using RWG basis functions [10-11].) This may explain the convergence rates reported in Table 2, although the effect is not apparent for small target sizes. For the Galerkin-tested EFIE-D, the SCS convergence rate of O(h^2) is expected due to variational properties [8-9]. However, the point-tested SCS also always appears to converge at an O(h^2) rate, which is contrary to expectation (and different from what is observed for the surface EFIE using RWG basis functions and point testing [11]). Since the SCS is computed by actually integrating over the SWG basis functions, one should expect an O(h) convergence rate in the absence of some variational effect.

The author has also investigated two-dimensional volume integral equations using triangular cells, and has observed similar behavior for the TM EFIE with pulse basis functions, and the TE EFIE with RWG basis functions [12]. In both cases, internal field results are usually slightly better with point testing, while SCS results appear to be as good or sometimes better with point testing than with Galerkin testing.

It is also observed in Table 1 that the point-tested results exhibit an SCS error that is usually comparable or larger than the field error, while the Galerkin-tested SCS error is often much smaller than the field error. This observation seems to be in accordance with the Galerkin theory that predicts that the SCS error will be lower than field error [8-9]. However, for these results the point-tested field error is often substantially smaller than the Galerkin-tested field error, so there is no net improvement in SCS error with Galerkin testing.

Table 1: Approximate error levels when the average edge length is 0.1 dielectric wavelengths

ka	ε_r	Unknowns for Avg. Edge Length = 0.1 λ_d	Point-Tested E-Field Error	Galerkin E-Field Error	Point-Tested SCS Error	Galerkin SCS Error
1.0	3	2100	0.007	0.015	0.006	0.006
1.0	5	4500	0.006	0.020	0.005	0.009
1.0	7	7400	0.007	0.035	0.004	0.016
1.0	10	12,600	0.007	0.060	0.0035	0.035
0.35	10	540	0.011	0.008	0.03	0.0034
0.6	10	2700	0.005	0.01	0.009	0.005
1.0	10	12,600	0.007	0.06	0.003	0.035
1.5	10	42,700	0.009	0.03	0.02	0.1

Table 2: Approximate convergence rates for the internal electric field error

ka	ε_r	Point E-Field Error Rate	Galerkin E-Field Error Rate
1.0	3	Between h and h^2	O(h)
1.0	5	O(h^2)	Between h and h^2
1.0	7	O(h^2)	O(h^2)
1.0	10	O(h^2)	O(h^2)
0.35	10	O(h)	O(h)
0.6	10	Between h and h^2	O(h)
1.0	10	O(h^2)	O(h^2)
1.5	10	O(h^2)	O(h^2)

IV. CONCLUSION

Results suggest that for the most widely-used volume integral formulation, the expected benefit of Galerkin testing is not realized in practice for many targets. Galerkin testing imposes a significant additional cost (an order of magnitude) in terms of matrix fill time, while increasing the complexity of the required integrations since observer locations are often closer to source cells as a result of the iterated integrals. However, it seldom produces more accurate near fields and only occasionally produces more accurate far fields than point testing.

It was observed in [7] that the EFIE-H formulation usually outperforms the Galerkin

EFIE-D approach. That observation also applies here, for a wider range of target size and permittivity than considered in [7]. However, in many cases the point-tested EFIE-D outperforms the EFIE-H approach.

In conclusion, when compared to the Galerkin-tested EFIE-D approach [1], the point-tested EFIE-D formulation is more efficient, more accurate for near fields, and usually as accurate for far fields.

REFERENCES

[1] D. H. Schaubert, D. R. Wilton, and A. W. Glisson, "A tetrahedral modeling method for electromagnetic scattering by arbitrarily shaped inhomogeneous dielectric bodies," *IEEE Trans. Antennas Propagat*., vol. AP-32, pp. 77-85, Jan. 1984.

[2] A. F. Peterson, "A magnetic field integral equation formulation for electromagnetic scattering from inhomogeneous 3-D dielectric bodies," in *Proc. 5th Annual Review of Progress in Applied Computational Electromagnetics*, pp. 387-403, Mar. 1989.

[3] S. A. Carvalho and L. S. Mendes, "Scattering of EM waves by inhomogeneous dielectrics with the use of the method of moments and 3D solenoidal basis functions," *Microwave and Optical Technology Letters*, vol. 23, pp. 42-46, Oct. 1999.

[4] M. M. Botha, "Solving the volume integral equations of electromagnetic scattering," *J. Comp. Physics*, vol. 218, pp. 141-158, 2006.

[5] L. E. Sun and W. C. Chew, "A novel formulation of the volume integral equation for electromagnetic scattering," *Waves in Random and Complex Media*, vol. 19, pp. 162-180, 2009.

[6] J. Markkanen, C.-C. Lu, X. Cao, and P. Yla-Oijala, "Analysis of volume integral equation formulations for scattering by high contrast penetrable objects," *IEEE Trans. Antennas Propagat.*, vol. 60, pp. 2367-2374, May 2012.

[7] A. F. Peterson, "Efficient solenoidal discretization of the volume EFIE for electromagnetic scattering from dielectric objects," *IEEE Trans. Antennas Propagat*., vol. 62, pp. 1475-1478, Mar. 2014.

[8] S. Wandzura, "Optimality of Galerkin method for scattering computations," *Microwave Opt. Technol. Lett.*, vol. 4, pp. 199-200, Apr. 1991.

[9] A. F. Peterson, D. R. Wilton, and R. E. Jorgenson, "Variational nature of Galerkin and non-Galerkin moment method solutions," *IEEE Trans. Antennas Propagat.*, vol. 44, pp. 500-503, Apr. 1996.

[10] A. F. Peterson, "Beyond RWG/Galerkin solutions of the EFIE: investigations into point-matched, discontinuous, and higher order discretizations," *Proceedings of the 27th Annual Review of Progress in Applied Computational Electromagnetics*, Williamsburg, VA, pp. 117-120, Mar. 2011.

[11] A. F. Peterson, "Observed baseline convergence rates and superconvergence in the scattering cross section obtained from numerical solutions of the MFIE," *IEEE Trans. Antennas Propagat*., vol. 56, pp. 3510-3515, Nov. 2008.

[12] A. F. Peterson, "Assessment of Galerkin testing for volume integral equations of electromagnetics," *Proceedings of the 30th Annual Review of Progress in Applied Computational Electromagnetics*, Jacksonville, FL, pp. 566-570, Mar. 2014.

[13] A. F. Peterson, "Volume integral equations for electromagnetic scattering from dielectric objects: observations and questions," *Forum for Electromagnetic Research Methods and Application Technologies (FERMAT)*, vol. 5, 10 pages, Sep.-Oct. 2014. (www.e-fermat.org)

Andrew F. Peterson received the B.S., M.S., and Ph.D. degrees in Electrical Engineering from the University of Illinois, Urbana-Champaign in 1982, 1983, and 1986 respectively. Since 1989, he has been a member of the faculty of the School of Electrical and Computer Engineering at the Georgia Institute of Technology, where he is now Professor and Associate Chair for Faculty Development. Within ACES, he has served at various times as a member of the Board of Directors, the Finance Committee Chair, the Publications Committee Chair, and the President. He also served as a Technical Co-Chair for the 25th Annual Review of Progress in Applied Computational Electromagnetics (ACES 2009). He was elevated to ACES Fellow in 2008.